

# Characterization of wind-induced vibrations in transmission lines by single-channel field data analysis

Hiroki Yamaguchi<sup>†</sup>, Chandra B. Gurung<sup>‡</sup>

*Department of Civil and Environmental Engineering, Saitama University, Shimo-Ohkubo 255,  
Sakura-Ku, Saitama 338-8570, Japan*

Teruhiro Yukino<sup>‡†</sup>

*Technical Research Center, Kansai Electric Power Co., Nakoji 3-11-20, Amagasaki 661-0974, Japan  
(Received January 13, 2004, Accepted September 21, 2004)*

**Abstract.** Wind-induced vibrations measured in the Tsuruga Test Line are characterized in this paper by single-channel data analysis based on piecewise application of Prony's method. Some of events were identified as galloping, while most of events were buffeting responses, which were confirmed partly by the buffeting analysis. Effects of end condition etc. on the response characteristics are also discussed.

**Keywords:** galloping; buffeting; transmission line; bundled conductors; Prony's method; single-channel field data.

---

## 1. Introduction

The term galloping is one of the common and very old terms in the field of overhead transmission line vibration during ice storm, and numerous research programs have been mounted over the years. Many researchers come up with various mathematical descriptions of phenomenon, mechanism and solution to prevent or at least minimize its effect. In spite of years of many theoretical studies, wind tunnel tests, and considerable field experiences, however, the notion of correctly observing and interpreting the actual galloping events in field still remains a challenge. On the contrary, any form of large amplitude vibration in ice storm is commonly regarded as galloping without identifying whether such oscillation is self-excited modal response.

In order to discuss galloping of transmission lines based on field data, a method of single channel signal processing has been implemented in the previous papers (Gurung, *et al.* 2001, 2002) for selective events. In this paper the same method is extended to identify and characterize several numbers of vibration observed in the Tsuruga Test Line of Kansai Electric Power Co. (KEPCO) during ice storms.

---

<sup>†</sup> Professor, Corresponding Author, E-mail: [hiroki@post.saitama-u.ac.jp](mailto:hiroki@post.saitama-u.ac.jp)

<sup>‡</sup> Formerly Graduate Student

<sup>‡†</sup> Senior Researcher

Based on the theory, galloping is defined as self-excited modal response, in which displacement response is most likely dominated by the action of galloping mode. Therefore, presence of single dominant harmonic component in displacement response, which can have time varying damping ratio and amplitude in unsteady wind but constant frequency, can represent galloping event. In this paper, after discussing time-averaged characteristics of responses obtained by spectral analysis, piecewise application of Prony's method is introduced to discuss time-dependent characteristics of harmonic components in the responses. The existence of motion-induced force is then confirmed for galloping events by introducing the usual buffeting theory. Finally, comparative discussions on buffeting response observed in different geometry of the Tsuruga Test Line sections are made.

## 2. Outline of Tsuruga test line and field measured data

The Tsuruga Test Line is located near the Tsuruga bay. The test line runs along the east-to-west mountain ridge in the Tsuruga area. The place has one of the typically severe metrological conditions in winter, which favors galloping of overhead transmission lines. The line sections are exposed to strong northwest winter wind blowing from Japan Sea (the Tsuruga bay) to Biwa Lake, which intercept the line sections nearly at right angle.

Fig. 1 shows the top view of the Tsuruga Test Line. There are three types of line sections namely, Phase A, Phase B and Phase C. Phase A and Phase B are two semi-suspension spans (one anchorage support and other suspension support at each span) line sections, where as, Phase C is two deadend span (both anchorage support at each end of the span) line section. Phase A and Phase B consist of six and four bundle conductors, respectively, while Phase C has two types of bundle configuration in each span. One span has six bundle conductors and the other consists of eight bundle conductors. The diameter of the bundle in Phase B is 0.5 m, while that for Phase A and Phase C is 2.6 m, which is very large as compared to usual size used in practice. The detail geometrical descriptions of each line section are shown in Table 1 (Yukino, *et al.* 1995).

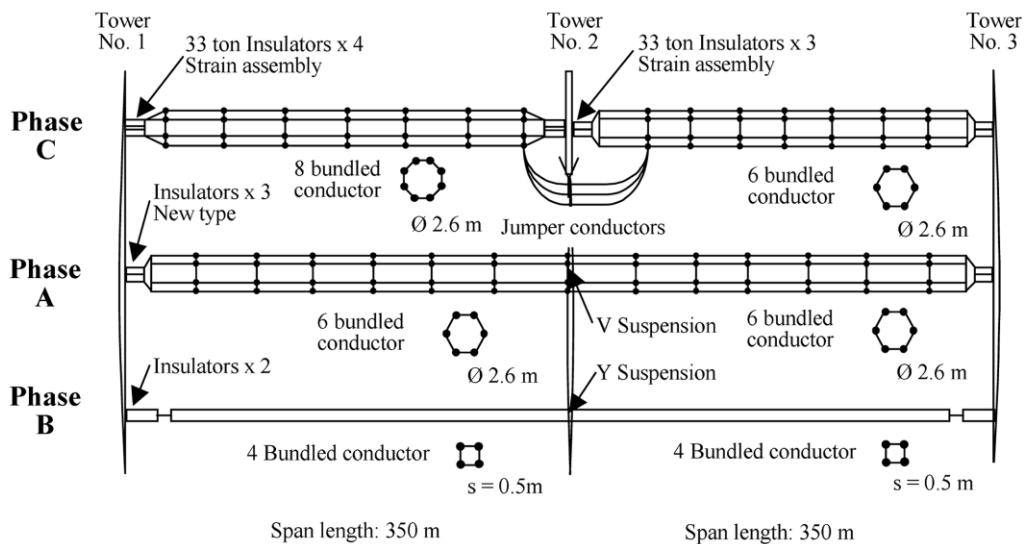
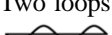


Fig. 1 Top view of the Tsuruga Test Lines, KEPCO

Table 1 Descriptions of the Tsuruga Test Lines

Description	Phase A	Phase B	Phase C
No. of conductors	6	4	6/8
No. of spans	2	2	1
Span length (m)	348×2	347×2	344
Sag to span ratio	0.041	0.037	0.042
<i>Per single conductor</i>			
Unit mass (kg/m/conductor)	3.35	3.35	3.35
Axial rigidity (MN/conductor)	65.2	65.2	65.2
Conductor diameter (mm)	30	38.4	30
Conductor spacing (m)	1.3	0.50	1.3

Table 2 Dynamic characteristics of the Tsuruga Test Lines

Motion	Mode/span	Phase A	Phase B	Mode	Phase C
		Freq. (Hz)	Freq. (Hz)		Freq. (Hz)
Horizontal	One loop 	0.14	0.14-0.15	One loop 	0.14
	Two loops 	0.28	0.28-0.315	Two loops 	0.281
	---	---	---	Three loops 	0.422
Vertical	One loop (up-down) 	0.157	0.166, 0.284	Quasi-one loop 	0.349-0.469
	One loop (up-up) 	0.28	0.288-0.320	Two loops 	0.275-0.315
	Two loops 	---	0.280-0.312	Three loops 	0.470-0.375
Torsion	One loop	0.148	---	One loop	0.125-0.148
	Two loops	0.29	0.28-0.386	Two loops	0.225-0.297
	---	0.44	---	Three loops	0.375-0.444

Dynamic characteristics of each line section are shown in Table 2 (Yamaguchi, *et al.* 1997). The mode of vibration is expressed in terms of number of loops per span. The fundamental mode of vibration in out-of-plane motion is single loop for all the phases. In in-plane motion, however, dynamic tension head during each mode of vibration governs the fundamental mode. Contrary to single loop mode in case of Phase A and Phase B, Phase C has two-loops mode as the fundamental mode in in-plane motion. It is due to the fact that single loop per span doesn't exist in deadend span because it requires an additional dynamic tension head. Quasi-single loop per span is the lowest order symmetric mode in Phase C, which has the frequency higher than that of two-loops mode. The single loop mode in Phase A and Phase C are up down and vice versa in respective spans.

The displacements were measured during vibrations at the quarter, mid and third quarters of the span in later years of observations. In order to measure the displacements, lamps are placed in the

transmission lines and video pictures of them were taken during vibrations. The pictured image is then converted to the digital data of horizontal and vertical components of displacement by data converter. In this paper, the single-channel data of thus digitized displacements at the quarter span are analyzed for characterizing the measured wind-induced vibrations in 1997 and 1998.

### 3. Spectral analysis

In order to study the measured responses based on their time-averaged characteristics, power spectra of responses at the quarter span, are first constructed and discussed. Fig. 2 depicts the power spectra of horizontal (or lateral) and vertical displacements in Phases A, B and C. As can be seen from Fig. 2(1), there is a large contribution of low frequency component in the horizontal responses of all the phases, which is a quasi-static response due to highly concentrated energy of wind at low frequency ranges as shown in the power spectra of wind velocity in Fig. 3. Such quasi-static response is significant and peculiar to transmission line structures because of their high flexibility especially in the lateral direction, and no particular difference can be seen in overall characteristics

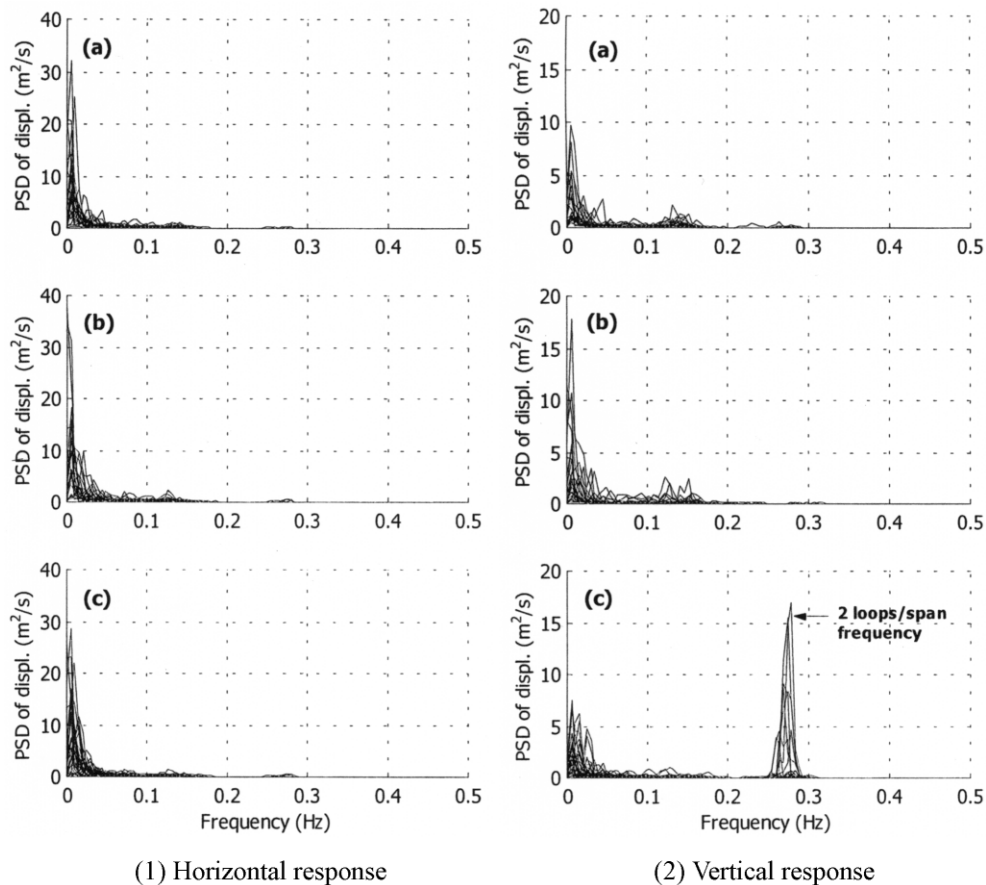


Fig. 2 Power spectra of (1) horizontal response and (2) vertical response at 1/4 span: (a) Phase A, (b) Phase B, and (c) Phase C.

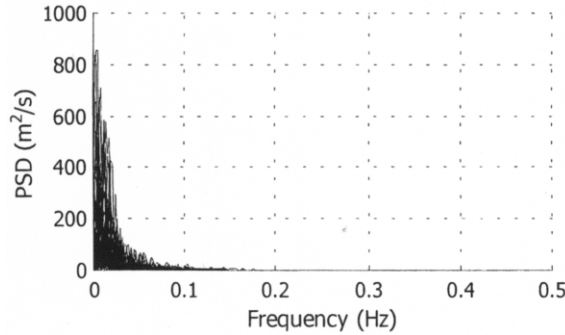


Fig. 3 Power spectra of horizontal wind velocity

of power spectra of horizontal responses. On the contrary, the spectra of vertical responses in Phase C are significantly different from other phases as shown in Fig. 2(2). There is a clear peak at a frequency close to the natural frequency of two-loops/span in-plane mode, which is well separated from the energy-concentrated range of wind spectra. This peak response at the modal frequency could be galloping, but the discussion is based only on the time-averaged characteristics. Prony-based decomposition is, therefore, applied in piecewise fashion in order to check the possibility of galloping by studying time-dependent response characteristics.

#### 4. Single-channel data analysis

##### 4.1. Prony-based exponential decomposition

Prony-based exponential decomposition is a method of decomposing a small time segment of signal into linear combination of exponential functions (components) similar to Fourier and Pisarenko's method. Applying Prony's method, a small time segment of signal can be modeled as:

$$\hat{x}(t) = \sum_{i=1}^N B_i e^{\lambda_i t} \quad (1)$$

where  $\hat{x}(t)$  is an estimated signal by Prony's method,  $B_i$  is the  $i$ -th weighing factor or the complex amplitude and  $e^{\lambda_i t}$  is the  $i$ -th exponential function. The Prony's method is usually applied to free vibration response in order to identify modal parameters, while the method is applied to the wind-induced response for identifying the dominant harmonic component with continuous frequency, or galloping component, in this study. Furthermore, the Prony-based exponential decomposition is applied in piecewise fashion in order to study time-dependent behaviors of harmonic components in the response. It is noted that the quasi-static component of response, which is gust response due to slowly varying wind speed, is filtered out by using highpass filter before applying the Prony's method.

Each time series of response is divided into pieces of 40 second segments as shown in Fig. 4 and the Prony's method is applied to each segment to estimate amplitudes, frequencies and damping ratios of harmonic components. In order to avoid ill conditioning of characteristics equation, the singular value decomposition is carried out to select an appropriate model order in the Prony's method. In each segment, dominant harmonic component, which is defined as the harmonic component with

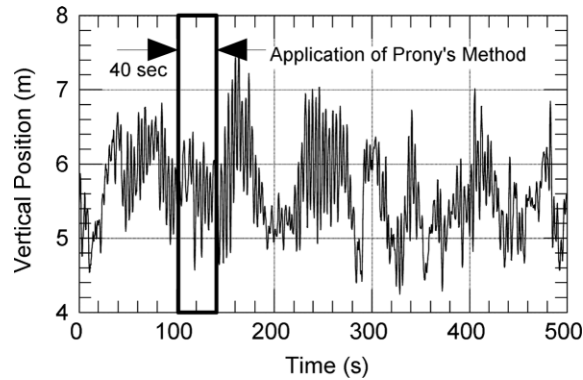


Fig. 4 A time series of vertical response in typical event: Phase C (6-bundle conductor), mean speed of 17.5 m/s

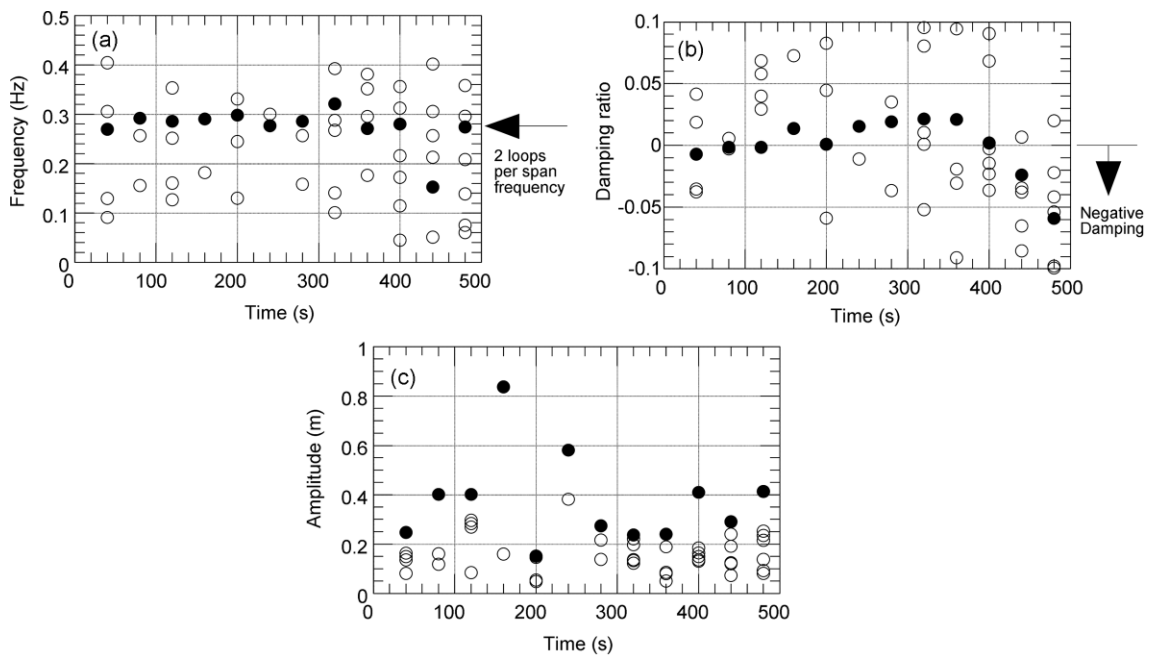


Fig. 5 Changes in (a) frequency, (b) damping ratio, and (c) amplitude of harmonic components identified by Prony's method in the vertical response data: (●) dominant component

the largest RMS value, is identified. The harmonic components identified for the time series in Fig. 4 by the piecewise application of Prony's method are depicted, as examples, in Fig. 5 where the identified frequency, damping ratio and amplitude of harmonic components are plotted with respect to the time. The time series of response, which has dominant harmonic components with frequency correlated over the time as clearly shown in Fig. 5(a), represents the galloping component as discussed in the previous paper (Gurung, *et al.* 2001, 2002). The correlated frequency is close to one of natural frequencies of the transmission line.

The discussion based only on the result of Prony's method, however, cannot explain whether the motion-induced force has augmenting effect to periodic motion to be called galloping. There might

be a possibility of dominant harmonic component with a correlated frequency due to dynamic amplification of the buffeting force. Therefore, an event with a dominant harmonic component with frequency constant over the time is separated and average amplitude of the dominant harmonic component is calculated for the event.

#### 4.2. Buffeting response analysis

The resonant response component of buffeting is next calculated and compared with the average amplitude of dominant harmonic component in order to ensure amplifying action of motion-induced force to periodic motion. The RMS of modal resonant component of buffeting is obtained for different mean wind speed by using Eq. (2):

$$\sigma_{Ri}^2 = \frac{1}{8[\zeta_{is} + \zeta_{ia}]} \left[ \frac{(\rho U C_L B)^2 S_u(f_i) |J(f_i)|^2}{\mu_i^2 (2\pi f_i)^3} \right] \quad (2)$$

where  $\sigma_{Ri}^2$ : mean square of resonant response component,  $\rho$ : mass density of air,  $C_L$ : aerodynamic lift force coefficient,  $U$ : mean wind speed,  $B$ : characteristic length of conductor,  $\zeta_{is}$ : structural damping ratio of the  $i$ -th mode,  $\zeta_{ia}$ : aerodynamic damping ratio of the  $i$ -th mode,  $\mu_i$ : the  $i$ -th modal mass,  $f_i$ : the  $i$ -th modal frequency,  $S_u(f_i)$ : value of power spectrum of wind at  $f_i$  frequency, and  $|J(f_i)|$ : joint acceptance function of the  $i$ -th mode.

In calculating the theoretical buffeting curves of modal resonant components, Simiu wind spectrum model (Simiu 1974), and the joint acceptance function suggested by Davenport (1962) are used. As is apparent from Eq. (2), the buffeting response is very much dependent on the modal damping, which is sum of structural and aerodynamic damping ratios, and the aerodynamic lift force coefficient, which is a function of the wind attack angle and the shape of ice-accretion. Both the shape of ice-accretion and the angle of wind attack vary for event-to-event and it is impossible to generalize these parameters by single values. Therefore, the buffeting analysis is carried out for the expected upper and lower values of modal buffeting response. The lift force coefficient, the modal damping ratio and the turbulence intensity are taken as 0.8, 1%, and 20%, respectively for the upper bound, and 0.2, 2% and 10%, respectively for the lower bound of buffeting response, which have been chosen based on the experimentally measured data by wind tunnel tests, the structural damping data by field vibration tests and the field measured data of wind.

It should be noted that there can be a significant contribution to the modal buffeting response from vertical component of turbulent wind in the case that the derivative of lift coefficient is large, which is possible under some conditions as shown later in Fig. 11. However, general discussion on the effect of vertical turbulence is also difficult and the buffeting response generated only by the horizontal turbulence is calculated in this paper by Eq. (2) for rough estimation of analytical buffeting curve.

## 5. Time-dependent characteristics of responses

### 5.1. Average amplitude and analytical buffeting curve

Because the amplitudes of the dominant harmonic component with the correlated frequency are

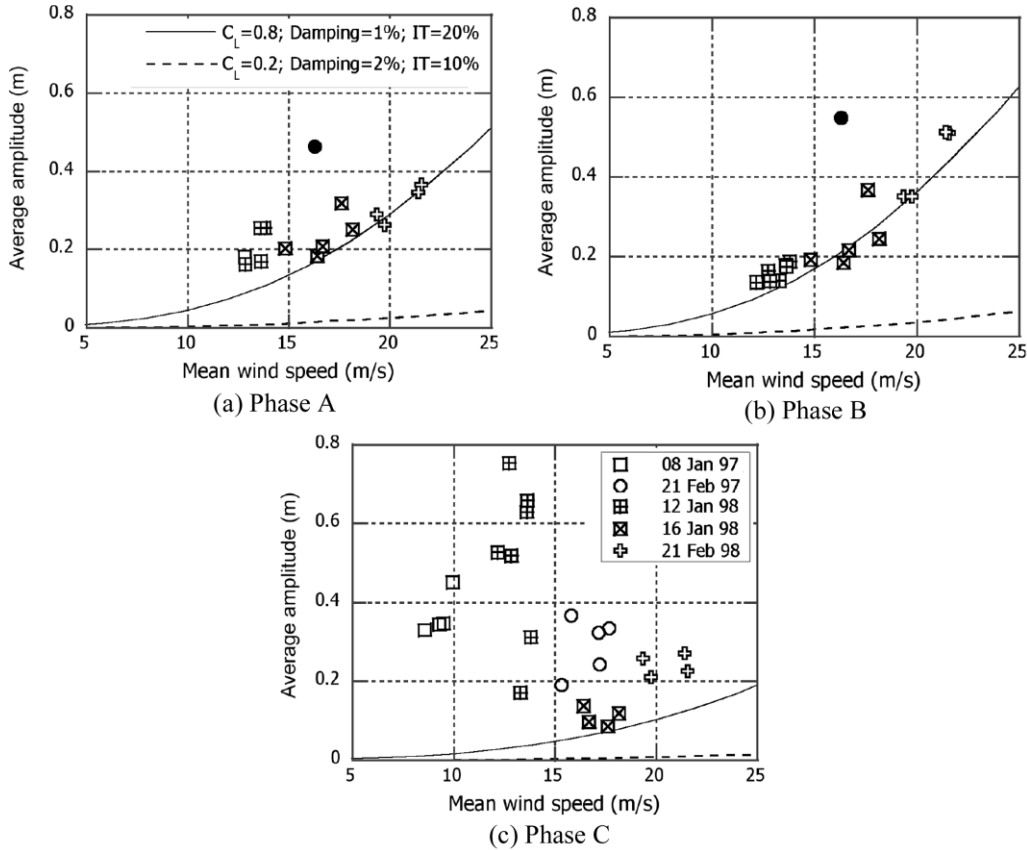


Fig. 6 Average amplitude in the vertical direction vs. mean wind speed

dependent on the time in each event, as shown in Fig. 5(c), their average is taken and plotted in Fig. 6 with respect to the event's mean wind speed. The events, which were observed in the same day but different period, are grouped together and depicted with same symbol. Similarly, the upper and lower limits of modal resonant component of buffeting were evaluated by using Eq. (2) and are compared with the average amplitude of dominant harmonic component.

As can be seen from Figs. 6(a) and (b), the average amplitudes of dominant harmonic components in Phase A and Phase B are consistent with the parabolic buffeting curve for the upper bound with an exception of the event depicted by (●). Therefore, while there are dominant harmonic components with frequency constant over the time, these events can be resulted from the modal response of buffeting. As for the exceptional event, this could have been galloping as it is far from the general trend of buffeting response, but it is unreliable to draw conclusion based on just a single event. In fact, the turbulent intensity of wind in this event is exceptionally large as shown in Fig. 7, and it can be concluded that the higher value of average amplitude in this event is partly contributed by the higher turbulent intensity of wind.

On the contrary, the average amplitudes of dominant harmonic components in Phase C, particularly with mean wind speed less than 15 m/s, do not follow any parabolic trend of buffeting response as shown in Fig. 6(c). The average amplitudes in these events are significantly higher than RMS of resonant response due to buffeting force, which indicates that there is an amplifying action

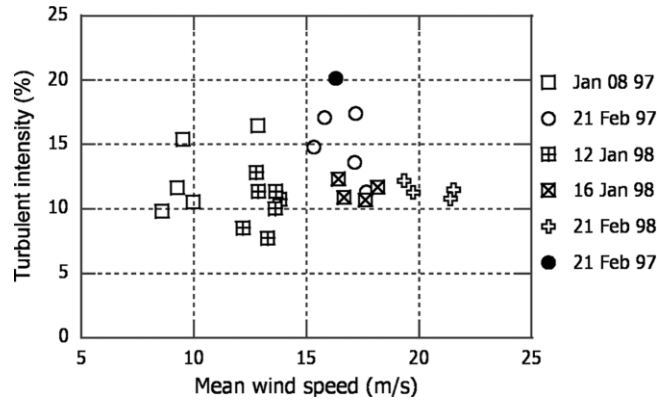


Fig. 7 Turbulence intensity in the horizontal direction vs. mean wind speed

of motion-induced force. Therefore, these events can be confirmed as galloping satisfying the characteristics of galloping, namely the presence of dominant harmonic component with frequency constant over the time and the amplifying action of motion-induced force.

### 5.2. Frequency and damping ratio of galloping

The average frequency of dominant harmonic component for the events in Phase C is depicted in Fig. 8. It can be seen from the figure that the galloping frequency for the lower mean wind speed is close to that of the first fundamental frequency of in-plane, two-loops/span mode in Table 2. In the case of higher mean wind speed, on the contrary, the frequency of dominant harmonic component is less than the fundamental in-plane frequency but close to the fundamental frequency of out-of-plane, one-loop/span mode in Table 2, indicating the possibility of swinging buffeting response in the out-of-plane mode.

The corresponding average damping ratio is depicted in Fig. 9, where not only the galloping events in the lower mean wind speed but also the buffeting events in the higher mean wind speed exhibit very low damping. While the damping ratio obtained by Prony-based exponential decomposition doesn't exclude the effect of excitation, the low average damping ratio less than the structural

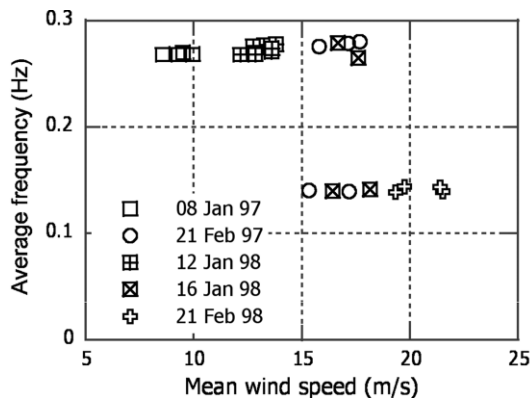


Fig. 8 Average frequency of vertical response vs. mean wind speed: Phase C

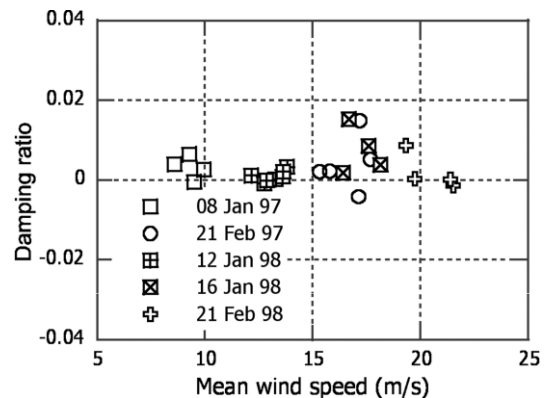


Fig. 9 Average damping ratio of vertical dominant mode vs. mean wind speed: Phase C

damping ratio, which is in the order of 1% (Yukino and Kuze 2001), can be due to a negative aerodynamic damping effect.

### 6. Possible causes of galloping

In summary of the previous discussions, galloping is observed only in Phase C, while all the phases are situated at the same location and subjected to the same ice storms over the observation period. This indicates the fact that the deadend span of Phase C is more prone to galloping than the semi-suspension spans such as Phase A and Phase B. Possible causes of galloping, which can be aerodynamic as well as mechanical ones, are discussed below more in detail by considering the shape of ice-accretion and the associated torsional response.

#### 6.1. Shape of ice-accretion

The approximate shapes of ice-accretion on 12 January 1998, when the distinct galloping events were observed in Phase C, were sketched at the time of field measurements for Phase B and Phase

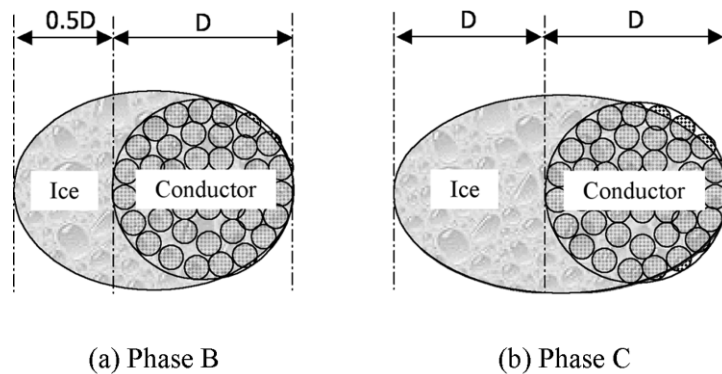


Fig. 10 Typical shape of ice-accretion

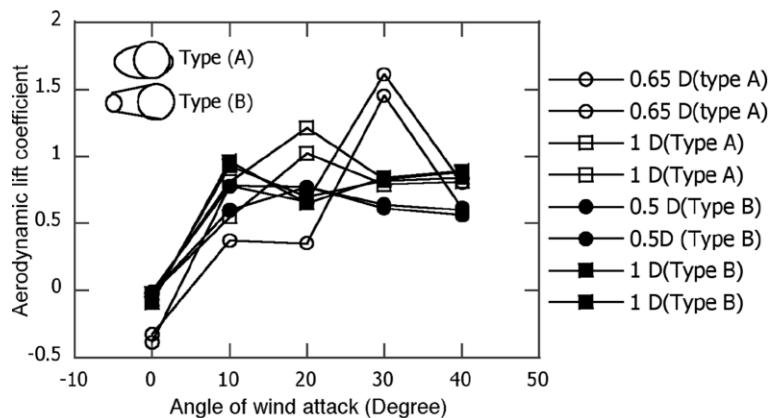


Fig. 11 Aerodynamic lift force coefficients for different ice-accretions

C as depicted in Fig. 10. It is clearly seen that more eccentric ice was accreted in Phase C than in Phase B. This might be due to the fact that Phase C with deadend span is stiffer than Phase B with semi-suspension span so that there is less gradual quasi-static rotation at the time of ice-formation. In order to compare the aerodynamic characteristics of different ice-shapes corresponding to Fig. 10, measured values of lift coefficients in wind tunnels are collected from the literature in Fig. 11. It can be learned from the figure that the aerodynamic coefficients are more significantly influenced by the angle of wind attack than the shape of ice-accretion. This fact can also be confirmed from the work of Keutgen (1998).

The angle of wind attack is mostly governed by the initial orientation of ice-accretion and the blow angle. While the information on the initial orientation of ice-accretion is not available, the blow-back angle in Fig. 12, obtained from the measured response, can be used to discuss effects of the wind attack angle on the galloping to some extent. Assuming that the angle of wind attack is in proportion to the blow-back angle, Den Hartog's instability criterion has been checked and it is found that there is a possibility of occurring Den Hartog's instability only in the events of Phase A and in the

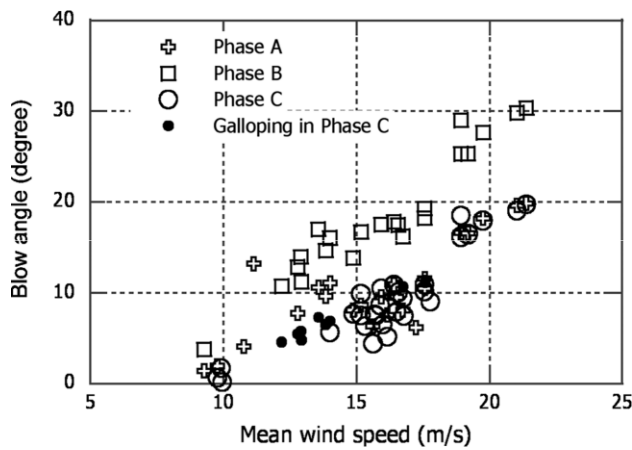


Fig. 12 Blow angles in Phase A, Phase B, and Phase C at 1/4 span

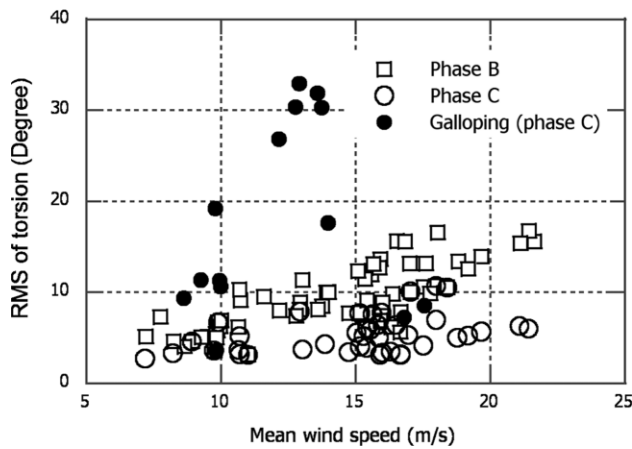


Fig. 13 Root mean square of torsional response at 1/4 span

non-galloping events in Phase C. It is, therefore, understood that the aerodynamic conditions due to eccentric ice formation in deadend span cannot be a sole cause of galloping in Phase C.

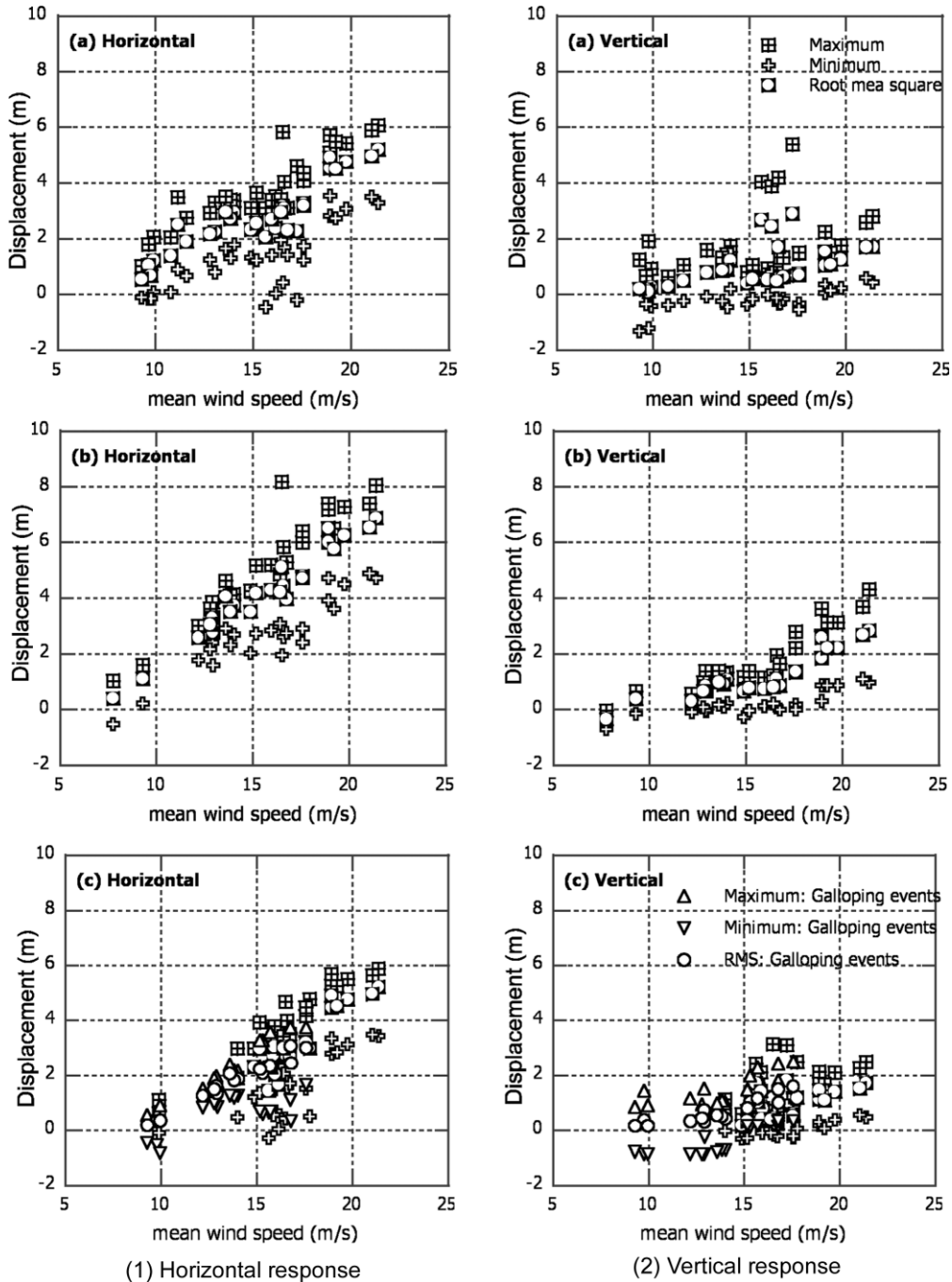


Fig. 14 Maximum, minimum and root mean square of response at 1/4 span: (a) Phase A, (b) Phase B, and (c) Phase C.

## 6.2. Torsional response

The RMS values of torsional response at the quarter span for the events measured by a gyroscope in Phases B and C are shown in Fig. 13. As can be seen in the figure, the galloping events are accompanied by excessive torsional responses especially at lower to moderate mean wind speed. It indicates the fact that the galloping can be due to coupled vertical and torsional motions rather than the sole aerodynamic condition. Since this study is based on the single-channel data analysis, the characteristics of coupled motion cannot be discussed and multi-channel data analysis is indispensable to study more on the mechanism of galloping in bundle transmission lines (Gurung, *et al.* 2003).

## 7. Buffeting responses

The possible maximum amplitudes of galloping and buffeting responses govern a rational design of phase clearance both in the vertical and horizontal directions. Therefore, the maximum, minimum and RMS values of horizontal and vertical responses observed in different phases have been evaluated directly from all the measured data and plotted in Fig. 14. As is expected, the horizontal response in Phase B, which has four conductors with smaller size bundles, is higher than that in Phase A and Phase C reaching to 8 m for the mean wind speed slightly higher than 20 m/s.

As for the vertical responses, Phase B has comparatively higher responses than Phase A and Phase C, while the vertical response in Phase A is slightly higher than that in Phase C. Furthermore, it is to be noted that the events in Phase C, which are identified as galloping, don't exhibit larger amplitude than the other buffeting events. Of course, this doesn't mean that galloping amplitude in Phase C is always smaller than that of buffeting response.

## 8. Conclusions

Based on the results of single-channel data analysis and observation of field-measured wind-induced vibrations in the Tsuruga Test Line, the following conclusions can be drawn.

- (1) The Prony-based exponential decomposition of single-channel data supported by analytical buffeting curve is successful for the identification of galloping and buffeting response in the field measured wind-induced vibrations. That is, a galloping event can be identified by checking a presence of dominant harmonic component with a frequency constant over the time, the associated damping around zero or negative, and the amplitude significantly larger than the modal buffeting response.
- (2) Frequent cases of galloping events are confirmed in the deadend span as compared to the semi-suspension span, when both of them are subjected to wide range of same ice storms.
- (3) Insignificant effect of end condition is found in the horizontal response (approximately along wind response), while slightly higher vertical response (across wind buffeting response) is observed in semi-suspension span than in deadend span.
- (4) The galloping amplitude need not be always larger than the amplitude of buffeting response.

## References

- Davenport, A.G. (1962), "Buffeting of suspension bridge by storm winds", *J. Struct. Div.*, ASCE, **88**(3), 233-268.
- Gurung, C.B., Yamaguchi, H. and Yukino, T. (2001), "Identification of galloping and buffeting in transmission lines", *Proceedings of 4th International Symposium on Cable Dynamics, Montreal, Canada*, 211-218.
- Gurung, C.B., Yamaguchi, H. and Yukino, T. (2002), "Identification of large amplitude wind-induced vibration of ice-accreted transmission lines based on field observed data", *Eng. Struct.*, **24**(2), 179-188.
- Gurung, C.B., Yamaguchi, H. and Yukino, T. (2003), "Identification and characterization of galloping of Tsuruga Test Line based on multi-channel modal analysis of field data", *J. Wind Eng. Ind. Aerodyn.*, **91**(7), 903-924.
- Keutgen, R. (1998), "Galloping phenomena a finite element approach", Ph.D. Thesis, University of Liege, Belgium.
- Simiu, E. (1974), "Wind spectra and dynamic along wind response", *J. Struct. Div.*, ASCE, **100**(9), 1897-1910.
- Yamaguchi, H., Xie, X. and Yukino, T. (1997), "Galloping analysis of transmission lines with bundle conductors", *Proceedings of 3rd International Symposium on Cable Dynamics, Trondheim, Norway*, 61-66.
- Yukino, T., Fujii, K. and Hayase, I. (1995), "Galloping phenomena of large bundle conductors observed on the full-scale test line", *Proceedings of 1st International Symposium on Cable Dynamics, Liege, Belgium*, 557-563.
- Yukino, T. and Kuze, T. (2001), "Vibration characteristics in the long span 4 bundled conductors of transmission line", *Proceedings of 5th Asia-Pacific Conference on Wind Engineering, Kyoto, Japan*, 193-196.